Int. J. Heat Mass Transfer. Vol. 15, pp. 2143–2153. Pergamon Press 1972. Printed in Great Britain

EFFECTS OF FORCED FLOW AND VARIABLE PROPERTIES ON BINARY FILM CONDENSATION*

V. E. DENNY and V. J. JUSIONIS

University of California, Los Angeles, California 90024, U.S.A.

(*Received* 27 *July* 1971 *and in revised form* 7 *January* 1972)

Abstract—Analysis of laminar film condensation of binary vapor mixtures undergoing forced flow down a vertical flat plate is presented. The conservation equations representing the coupled two-phase flow problem are markedly nonsimilar and were solved numerically using a forward marching technique. The behavior of the liquid film was treated by means of a locally valid Nusselt-type analysis which provided interior boundary conditions for the vapor-side problem. Locally variable properties in the liquid phase were obtained from mixture data, the effects of temperature variations across the falling film being evaluated at appropriate reference temperatures. Vapor mixture properties were calculated from kinetic theory.

Heat transfer results in the form q/q_{Nu}, where q_{Nu} is the classical Nusselt solution for one of the pure species, are reported for the binary mixtures methanol–H_2O, propanol–H_2O, acetone–H_2O, and acetone–CCl_4. For non-azeotropic binary mixtures, it is found that q/q_{Nu} passes through minimum values as the bulk concentration of the more volatile component increases. The approach to the minimum is similar in behavior to the noncondensable gas problem, the magnitude of $q/q_{Nu}|_{min}$ being inversely proportional to the relative volatility of the binary pair. A second feature of binary film condensation is the first order dependence of the results for q/q_{Nu} on the composition of the liquid film via variable liquid properties. The effects of forced convection are similar to those observed for the noncondensable gas problem.

NOMENCLATURE

A, physical property group $= k_l^3 \rho_l \lambda / \nu_l$;
$\mathscr{B}$, mass transfer driving force;
C_p, heat capacity;
$\mathscr{D}_{12}$, binary diffusion coefficient;
g, standard gravitational acceleration;
g, mass-transfer conductance;
h, enthalpy;
j, mass diffusion flux;
k, thermal conductivity;
m, mass fraction;
$\dot{m}$, condensation rate per unit area $= \rho v|_s$;
p, partial pressure;
P, total pressure;
Pr, Prandtl number $= \mu C_p/k$;
q, heat flux;
q_{Nu}, Nusselt heat flux $= [k_l^3(T_e - T_w)^3 \rho_l g \lambda / 4 x \nu_l]^{\frac{1}{4}}$;
Re_x, Reynolds number $= u_e x/\nu_e$;
Sc, Schmidt number $= \nu/\mathscr{D}_{12}$;
T, absolute temperature;
u, v, velocity components;
x, y, boundary-layer coordinates.

Greek symbols

α, relative volatility $= p_1(T_s)/p_2(T_s)$;
δ, condensate film thickness;
ε, constant defined in equation (25);
η, suction parameter $= -\dot{m} Re_x^{1/2}/\rho_{v,e} u_e$;
λ, latent heat of vaporization;
μ, absolute viscosity;
ν, kinematic viscosity;
ρ, density;
τ, shear stress.

* This work was supported in part by the State of California through the University of California Statewide Water Resources Center and by the Department of the Interior. OSW Grant No. 14-30-2678. Computer time for the numerical computations was provided in part by the Campus Computing Network of the University of California, Los Angeles.

Subscripts

e.	at the vapor boundary-layer edge;
i.	at the vapor–liquid interface;
l.	in the liquid phase;
min.	minimum
s.	at the s–surface (see Fig. 1);
u.	at the u-surface (see Fig. 1);
v.	in the vapor phase;
w.	at the wall;
x.	at position x;
-1.	as $\mathscr{B} \rightarrow -1$;
1.	of the more volatile species;
2.	of the less volatile species.

Superscripts

*.	independent of x.

INTRODUCTION

IN A RECENT paper, Sparrow and Marschall [1] formulated a predictive theory for binary, gravity-flow film condensation on a vertical plate in the absence of forced convection. The analytical method was applied to condensation of saturated mixtures of methanol and water vapor at 1 atmosphere. Heat-transfer results in the form q/q_0, where q_0 is the Nusselt heat flux based on ambient conditions, exhibit a marked dependence on bulk composition and overall temperature difference. Strong minima in q/q_0 are found, at a bulk composition $m_{1,e} \doteq 0{\cdot}41$, whose magnitudes vary directly with overall temperature difference. At high condensation rates, a simplified computational procedure is developed which does not require solutions of the vapor-side boundary-layer equations.

Since the physical properties of liquid mixtures vary strongly with composition, it is of interest to examine further the problem of binary film condensation for other systems. In addition, as demonstrated in [1], the character of the results is intimately related to the nature of the vapor-equilibrium curve for a given binary pair. Thus, a fully predictive theory requires a broader spectrum of results in order that the combined effects of variable properties in the liquid phase and the diverse characteristics of vapor–liquid equilibria for various systems may be delineated. Furthermore, the usual industrial situation involves forced flow of the vapor phase. As demonstrated in [2] and [3], the effects of forced flow on the mass transfer conductance for condensation of pure vapors in the presence of a noncondensable gas has a marked influence on heat-transfer rates. Similar effects would be anticipated for binary film condensation, since the more volatile species would tend to behave like a noncondensable gas.

The objectives of the present paper are to investigate the effects of forced flow and variable physical properties on film condensation of methanol–H_2O, propanol–H_2O, acetone–H_2O and acetone–CCl_4. These systems were chosen because their thermo-physical properties encompass a variety of features which are encountered in practice. For example, aqueous mixtures of methanol and propanol exhibit strong maxima in liquid mixture viscosity. The propanol–water system additionally exhibits a minimum boiling azeotrope; while, saturated mixtures of acetone–CCl_4 are essentially isothermal over a broad range of composition. The acetone–water system exhibits a sharp

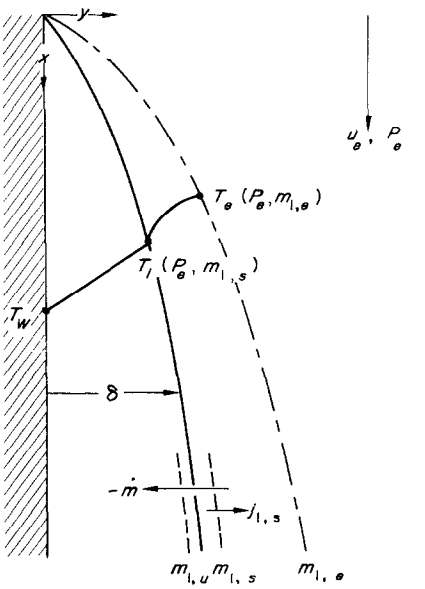

FIG. 1. Schematic of physical situation.

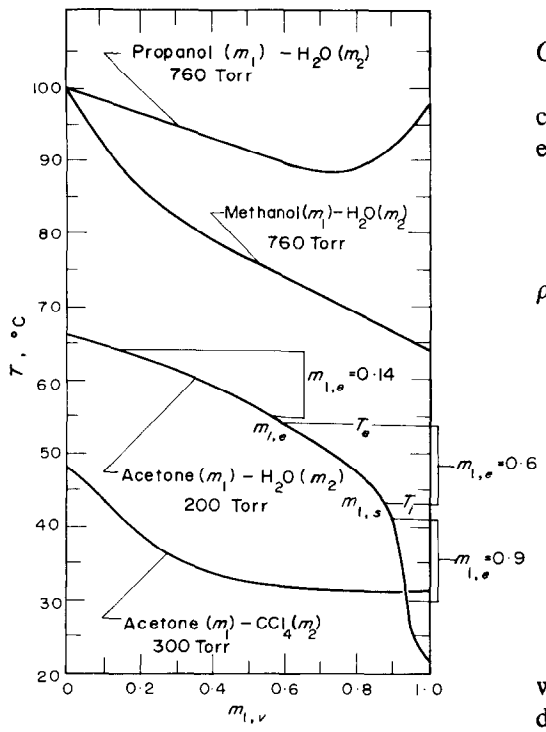

FIG. 2. Vapor-side equilibrium data with example of accumulation of more volatile species (m_1) at the s-surface (acetone–H_2O; x = 0·5 ft, u_e = 10 ft/s, $T_e - T_w$ = 20°F).

decline in equilibrium temperature as $m_{1,v} \to 1$ (see Fig. 2).

The physical situation involved is illustrated in Fig. 1. The vertical condenser surface is at a uniform temperature T_w. The coordinates along and normal to the surface are x and y, respectively, and the corresponding velocity components are u and v. At some distance from the surface, the [saturated] vapor mixture has composition $m_{1,e}$ and pressure P_e, and is flowing at a uniform velocity u_e. The temperature T_e is the dew point temperature for given P_e and $m_{1,e}$. The condensate film has thickness δ, which varies with x. At the vapor–liquid interface, the temperature T_i and, hence, the mass fraction $m_{1,s}$ (or, equivalently, $m_{1,u}$) are unknown and must be determined in the course of the analysis. Here, the s- and u-surfaces denote locations δ^+ and δ^-, respectively. With forced flow, T_i and $m_{1,s}$ are of course functions of x.

ANALYSIS

Governing equations and boundary conditions

For the vapor phase, the equations governing conservation of mass, momentum, species, and energy are, respectively,

$$\frac{\partial}{\partial x}(\rho_v u) + \frac{\partial}{\partial y}(\rho_v v) = 0 \tag{1}$$

$$\rho_v u \frac{\partial u}{\partial x} + \rho_v v \frac{\partial u}{\partial y} = \frac{\partial}{\partial y}\left(\mu_v \frac{\partial u}{\partial y}\right) + g(\rho_v - \rho_{v,e}) \tag{2}$$

$$\rho_v u \frac{\partial m_1}{\partial x} + \rho_v v \frac{\partial m_1}{\partial y} = \frac{\partial}{\partial y}\left(\rho_v \mathscr{D}_{12} \frac{\partial m_1}{\partial y}\right) \tag{3}$$

$$\rho_v u \frac{\partial T}{\partial x} + \rho_v v \frac{\partial T}{\partial y} = \frac{\partial}{\partial y}\left(\frac{k_v}{C_{p,v}} \frac{\partial T}{\partial y}\right) + \frac{k_v}{C_{p,v}} \frac{\partial T}{\partial y} \frac{\partial \ln C_{p,v}}{\partial y} + \frac{\rho_v \mathscr{D}_{12}}{C_{p,v}} (C_{p,1} - C_{p,2}) \cdot \frac{\partial m_1}{\partial y} \frac{\partial T}{\partial y} \tag{4}$$

where the second order effects of thermal diffusion, viscous dissipation, compressible heating, and diffusion-thermo have been neglected in equations (3) and (4).

For the liquid phase, the composition at the u-surface (see Fig. 1) is expected, for the nonsimilar problem under consideration here, to vary with x. Thus, an assumption of uniform composition throughout is not valid. However, when the full boundary-layer equations were employed to account for transport of momentum, mass species, and thermal energy in the liquid film, it was found [4] that the classical Nusselt assumptions, wherein convection of energy and momentum in all but low Prandtl number fluids may safely be neglected [5], can be extended in the present situation to include convection of mass species as well. (See Results and Discussion.) Thus, the defining equations in the liquid film are taken as

$$0 = \mu_l \frac{d^2 u}{dy^2} + g(\rho_l - \rho_{v,e}) \tag{5}$$

$$0 = \frac{d^2 T}{dy^2} \tag{6}$$

$$0 = \frac{d^2 m_1}{dy^2} \tag{7}$$

where, from equation (7), it is seen that the liquid-side composition is uniform across the liquid film since the wall is impermeable. The variable liquid properties are therefore evaluated locally at composition $m_{1,u}(x)$ and, following [5], reference temperature

$$T_r = T_w + \tfrac{1}{3}[T_i(x) - T_w]. \tag{8}$$

Equations (1)–(7) are subject to the boundary conditions

$$u \to u_e, \quad m_1 \to m_{1,e}, \quad T \to T_e \tag{9a}$$

as $y \to \infty$;

$$u = 0, \; dm_1/dy = 0, \; T = T_w \tag{9b}$$

at $y = 0$; and

$$u|_u = u|_s = u_i \tag{10}$$

$$T|_u = T|_s = T_i \tag{11}$$

$$\mu_l \left.\frac{\partial u}{\partial y}\right|_u = \mu_v \left.\frac{\partial u}{\partial y}\right|_s = \tau_i \tag{12}$$

$$\dot{m} m_1|_u = \dot{m} m_1|_s + j_{1,y}|_s = \dot{m} m_1|_s - \rho_v \mathscr{D}_{12} \left.\frac{\partial m_1}{\partial y}\right|_s \tag{13}$$

$$\dot{m} h|_u + q_y|_u = \dot{m} h|_s + q_y|_s \tag{14}$$

at the interface. Equation (13) may be written in the form

$$\frac{\rho \mathscr{D}_{12} (\partial m_1/\partial y)|_s}{m_{1,s} - m_{1,u}} = \dot{m} = -\frac{d}{dx} \int_0^\delta \rho u \, dy|_l \tag{15}$$

where, clearly, $\dot{m}_u = \dot{m}_s$. Equation (14) may be written as

$$k_l \left.\frac{\partial T}{\partial y}\right|_u = -\dot{m}(m_{1,u}\lambda_1 + m_{2,u}\lambda_2) + k_v \left.\frac{\partial T}{\partial y}\right|_s \tag{16}$$

provided the heats of solution are negligibly small. It is shown in [4] that the heats of solution for methanol and water contribute, at most, 3 per cent to the total heat load at the wall. Since the heats of solution for other binary pairs are comparably small, this effect was neglected throughout. In addition, it is presumed that the interface is in thermodynamic equilibrium. Thus, for a given total pressure,

$$T_i = T_i(m_{1,s}, P_e) \quad \text{and} \quad m_{1,u} = m_{1,u}(m_{1,s}, P_e). \tag{17}$$

Following Patankar and Spalding [6], equations (1)–(4) were solved by means of finite difference methods, iteration being required at each marching step to achieve compatibility with the liquid side problem. A detailed description of the overall numerical procedure is given in [4]. For the cases reported here, 100 node points were used across the vapor boundary layer and, as shown in [4], the maximum error in the heat transfer results is a few per cent.

Thermophysical properties

Experimental data for the mixture properties ρ_l, k_l, μ_l and λ were extracted from sources listed in [4] and fit with appropriate algebraic expressions. Vapor–liquid equilibrium data was taken from Landolt and Börnstein [7] and local interpolation used to relate $m_{1,u}$, $m_{1,s}$, and T_i. For the vapor-side transport coefficients, mixture rules as set forth by Mason and Monchik [8] were used to calculate, first $\mathscr{D}_{12}$ and, then, μ_v and k_v, assuming a Lennard–Jones interaction potential. Collision parameters were taken from Svehla [9]. Ideal gas behavior was assumed in the vapor, and the pure species values of μ, k and C_p were obtained from sources listed in [4]. A complete bibliography of data sources and calculational procedures appears in [4].

RESULTS AND DISCUSSION

The effects of forced flow (u_e), overall temperature drop ($T_e - T_w$), and free stream composition ($m_{1,e}$) on binary film condensation of methanol (m_1)–water (m_2), propanol (m_1)–water (m_2), acetone (m_1)–water (m_2), and acetone (m_1)–CCl_4 (m_2) have been investigated at the total pressures P_e = 760, 760, 200 and 300 Torr, respectively. (The values of P_e were dictated by available vapor–liquid equilibrium data.) Vapor-side equilibrium data, in the form T(°C) vs. mass fraction of the more volatile component ($m_{1,v}$),

are displayed in Fig. 2. Note that propanol–water exhibits a strong minimum boiling azeotrope ($T = 87{\cdot}76°C$, $m_{1,s} \equiv m_{1,u} = 0{\cdot}718$). acetone–$CCl_4$ is essentially isothermal over the range $0{\cdot}5 \leqslant m_{1,v} \leqslant 1{\cdot}0$ ($T = 31{\cdot}25°C$), and acetone–water exhibits sharply declining temperatures for $0{\cdot}88 \leqslant m_{1,v} \leqslant 1{\cdot}0$.

Typical heat transfer results are displayed in Figs. 4–10 where the local heat flux q, with the exception of the results in Fig. 10, has been normalized with respect to the classical Nusselt heat flux for film condensation of pure water vapor (the less volatile component), assuming the vapor to be saturated at ambient temperature T_e:

$$q_{Nu} = [k_l^3(T_e - T_w)^3 g\rho_l\lambda/4\nu_l x]^{\frac{1}{4}}. \qquad (18)$$

Over the range of conditions considered, $10^{-5} . Re_x$ ($x = 0{\cdot}5$ ft and $u_e = 100$ ft/s) typically equaled about 3·3, 2·3, 1·4 and 10, respectively for the systems cited above. Thus, the assumption of a laminar vapor boundary layer, with the possible exception of the 100 ft/s acetone–CCl_4 results, is sound. For the liquid film $4\Gamma/\mu_l$, where Γ is the mass flow rate per unit width of film at $x = 0{\cdot}5$ ft, ranged from 6·6–120, 43–120, 3–20 and 40–130, respectively. Again, the assumption of laminar flow is probably sound [10, 11]; although, at the higher film Reynolds numbers rippling most likely occurs [12]. Nonetheless, the results are not without value since they serve as base solutions for empirical correlations and future theoretical analyses of the effects of waves and turbulence.

The accuracy and credibility of the solution method are demonstrated in Figs. 3 and 4. The assumption of locally uniform composition in the liquid phase is supported by the results in Fig. 3 where solutions of the full boundary layer equations in both phases are compared with solutions obtained using equations (5)–(7) for the film. (The non-monotonic character of $T_i - T_w$ and m_1 near $x = 0$ is due to some degree of arbitrariness in assigning initial conditions [2].) Although the resistance to mass transfer is not inappreciable (compare solid

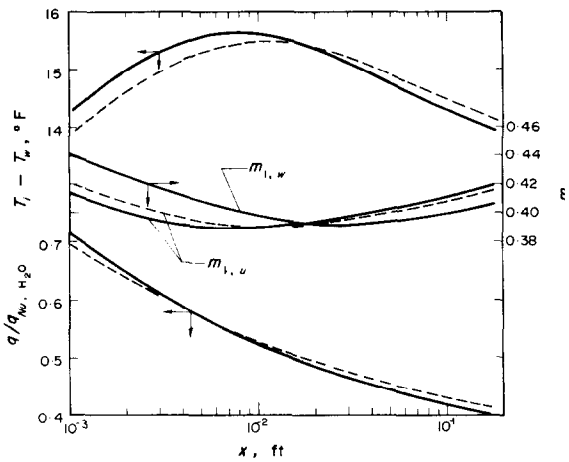

FIG. 3. Comparisons of results obtained using boundary layer forms of the liquid-side conservation equations (———) with those using equations (5)–(7) (– – –). Methanol (m_1)–water (m_2); $P_e = 760$ Torr, $m_{1,e} = 0{\cdot}5$, $u_e = 10$ ft/s, $T_e - T_w = 20°F$, $Sc_l \doteq 800$. Fifty node points across vapor boundary layer, 21 nodes across liquid film.

curves for $m_{1,u}$ and $m_{1,w}$), the results for q/q_{Nu} suggest that equations (5)–(7) are adequate for predicting heat transfer. This is a consequence in part of the near isothermal character of the interface—over the range of conditions treated here, $T_i(x)$ varied approximately 0·5°F on the average ($0{\cdot}05 \leqslant x \leqslant 0{\cdot}5$ ft), with a maximum change of about 3°F.

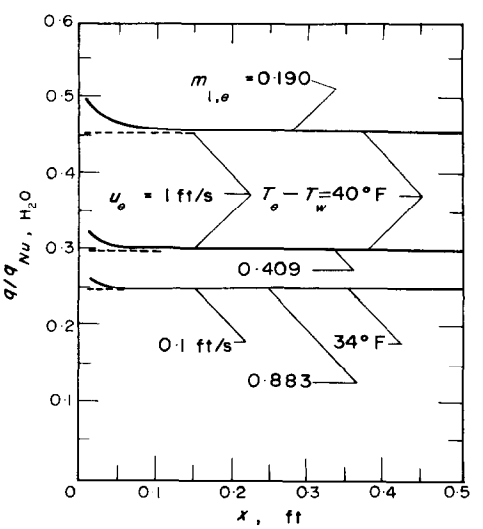

FIG. 4. Condensation of methanol–water mixtures at $u_e \to 0$ ($P_e = 760$ Torr); ——— this study, – – – [1].

In Fig. 4, results for methanol–water, with $u_e \to 0$ are compared with similarity solutions extracted from [1]. (Results were not obtained at $u_e = 0$ due to prohibitive computational cost.) Excepting a small region near $x = 0$, where nonsimilar effects are evident, the agreement is uniformly excellent. Even at 1 ft/s, the results quickly merge with the similarity solution. The latter result is not surprising since, as discussed in [1], the influence of streamwise convection on the convective flow field, for $u_e \to 0$, is relatively weak at the high interfacial mass transfer rates which obtain with $T_e - T_w$ so large.

With increasing u_e, the effects of forced convection are more pronounced (Fig. 5). Not

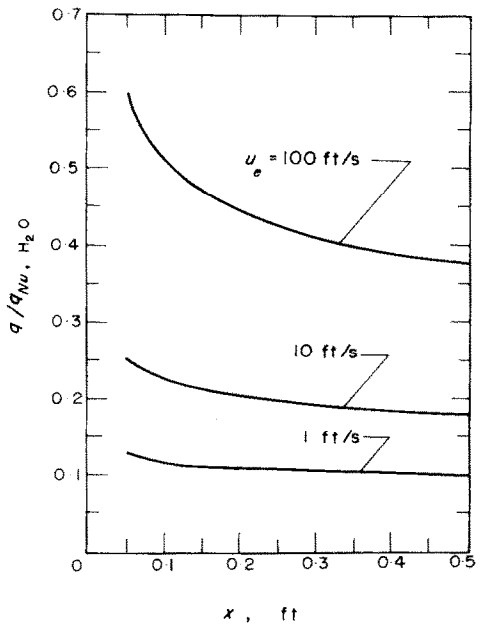

FIG. 5. Effects of u_e on condensation of methanol–water mixtures; P_e = 760 Torr, T_e = 197·5°F, $m_{1,e}$ = 0·409, $T_e - T_w$ = 20°F.

only does the level of q/q_{Nu} rise but also the physical situation becomes increasingly more nonsimilar. As discussed in [2] and [3], these effects are a direct consequence (i) of vapor drag, and (ii) enhancement of the mass-transfer conductance. For boundary layer flows undergoing strong suction, vapor drag is approximately equal to the asymptotic value $\dot{m}u_e$ and, since $\dot{m} \propto x^{-n} (n > 0)$, the effects of u_e on the liquid film thickness and, hence, q are self-evident.

From equation (15), there may be defined

$$\dot{m} = \frac{\rho \mathscr{D}_{12}(\partial m_2/\partial y)|_s}{(m_{2,s} - m_{2,u})} \equiv \mathscr{B}g \tag{19}$$

where

$$\mathscr{B} = (m_{2,e} - m_{2,s})/(m_{2,s} - m_{2,u}) \tag{20}$$

is the mass transfer driving force and

$$g = \rho \mathscr{D}_{12} \partial[m_2/m_{2,e} - m_{2,s})]/\partial y|_s \tag{21}$$

is the mass-transfer conductance. Paralleling arguments in [3], g may be expected to assume the form

$$g = C \cdot g_{-1} \cdot F(\eta) \tag{22}$$

where C is a constant.

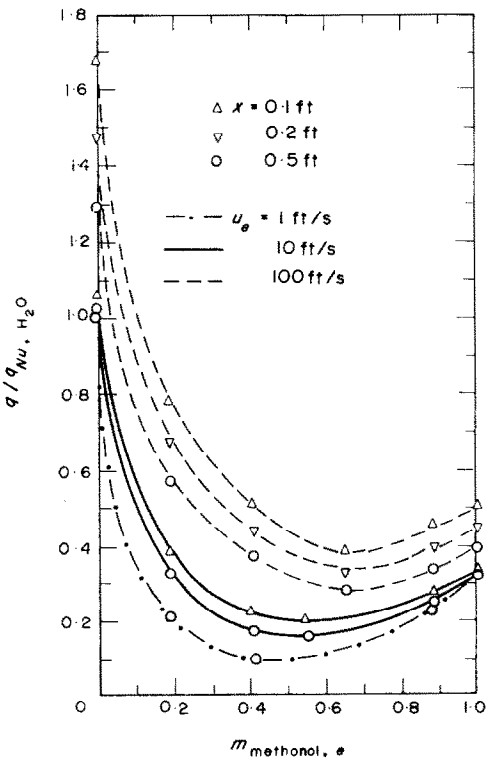

FIG. 6. Effects of $m_{1,e}$ and u_e on condensation of methanol–water mixtures; P_e = 760 Torr, $T_e - T_w$ = 20°F.

$$g_{-1} = \rho_{v,e} u_e Sc_e^{-1} Re_x^{-\frac{1}{2}} / [2(1 + \mathscr{B})(1 + Sc_e^{-1})]^{\frac{1}{2}} \quad (23)$$

is the similarity solution of Acrivos [13]. which applies in the limit $\mathscr{B} \to -1$. and $F(\eta)$ is a monotonic increasing function of the suction parameter [14]

$$\eta = q_{Nu} Re_x^{\frac{1}{2}} / \rho_{v,e} u_e \lambda . \quad (24)$$

For given x. $T_e - T_w$. and $m_{2,e}$, $g \propto u_e^{\frac{1}{2}}$ and one might expect an approximate 3-fold increase in $q = -\lambda \dot{m}$ for each 10-fold increase in u_e. provided $\mathscr{B}$ remained constant. However. at $x = 0{\cdot}3$ ft, $\mathscr{B}$ actually increased from $-0{\cdot}66$ to

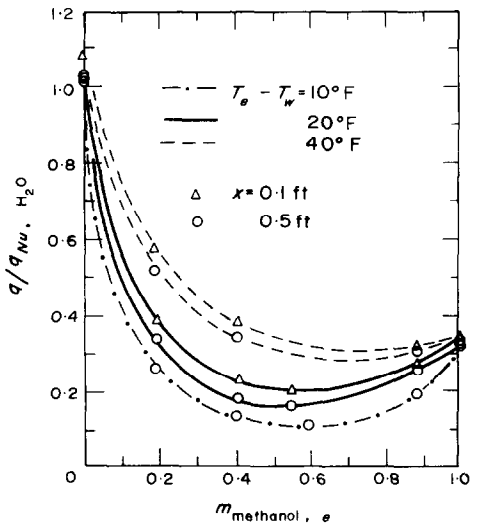

FIG. 7. Effects of $m_{1,e}$ and $T_e - T_w$ on condensation of methanol–water mixtures; $P_e = 760$ Torr. $u_e = 10$ ft/s.

$-0{\cdot}57$ as u_e increased from 10 to 100 ft/s. Thus $\mathscr{B}g|_{100}/\mathscr{B}g|_{10} \doteq 2{\cdot}5$. which compares favorably with the actual 2·2-fold increase exhibited in Fig. 5.

The effects of $m_{1,e}$ on film condensation of mixed vapors are displayed in Figs. 6–10. The predominant features of the results are (i) an initial rapid decline in q/q_{Nu} as $m_{1,e}$ increases. and (ii) minima in q/q_{Nu} for the non-azeotropic binary pairs. These trends are, to first order, related to physical property variations in the

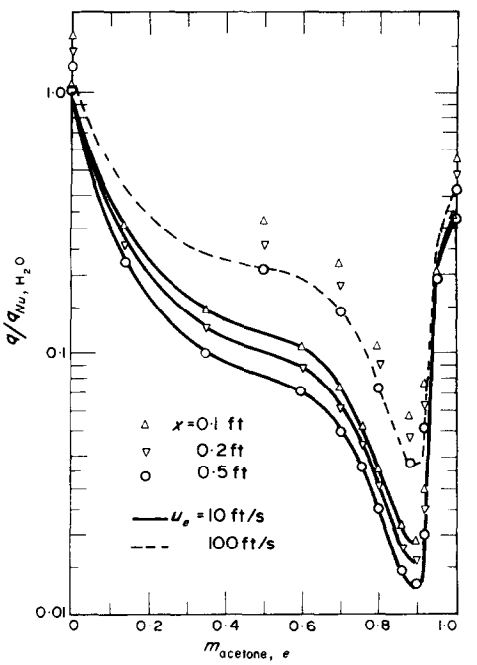

FIG. 8. Effects of $m_{1,e}$ and u_e on condensation of acetone–water mixtures; $P_e = 200$ Torr, $T_e - T_w = 20$°F.

liquid phase as well as to the nature of the vapor–liquid equilibrium curve. For given x and $T_i - T_w$. heat transfer across the liquid film is characterized by the physical property group $A \equiv k_l^3 \rho_l \lambda / \nu_l$ (see equation (18)). The ratio $(A/A_0)^{\frac{1}{4}}$. where A_0 is the larger of the values of A at the pure species end points, is presented in Fig. 11 for typical film temperatures. For the aqueous mixtures, k_l, ρ_l and λ decrease with increasing organic concentration ($m_{1,u}$) whereas μ_l exhibits strong maxima. Thus, $(A/A_0)^{\frac{1}{4}}$, where $A_0 = A_{m_{1,u}=0}$, initial decreases very rapidly as $m_{1,u}$ increases. However, for acetone–CCl_4, the much larger density of CCl_4 partially compensates for strong reduction in $k_l^3 \lambda / \mu_l$ with increasing $m_{CCl_4,u}$ and $(A/A_0)^{\frac{1}{4}}$ *increases* modestly with increasing $m_{1,u} = m_{acetone,u}$.

Returning to Fig. 2, it is seen that as [more volatile] species 1 accumulates at the s-surface (Fig. 1) due to convective inflow. $T_i(m_{1,s}, P_e)$ drops below T_e (see, for example, the saturated vapor curve for acetone (m_1)–H_2O(m_2)). This

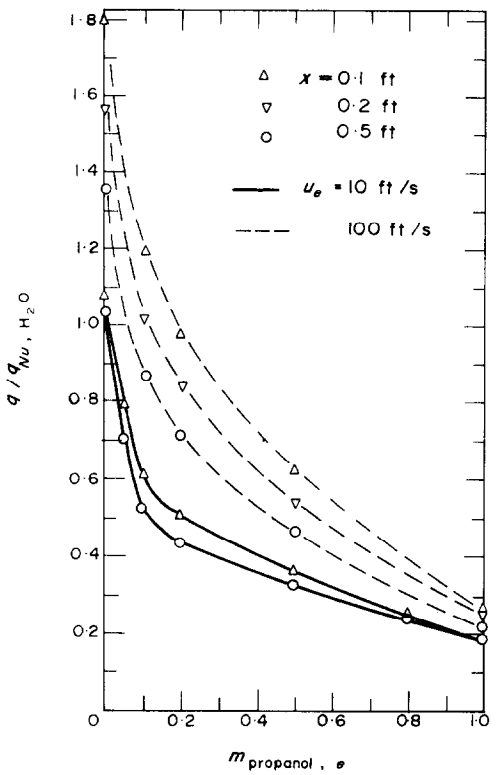

FIG. 9. Effects of $m_{1,e}$ and u_e on condensation of propanol–water mixtures; $P_e = 760$ Torr, $T_e - T_w = 20°F$.

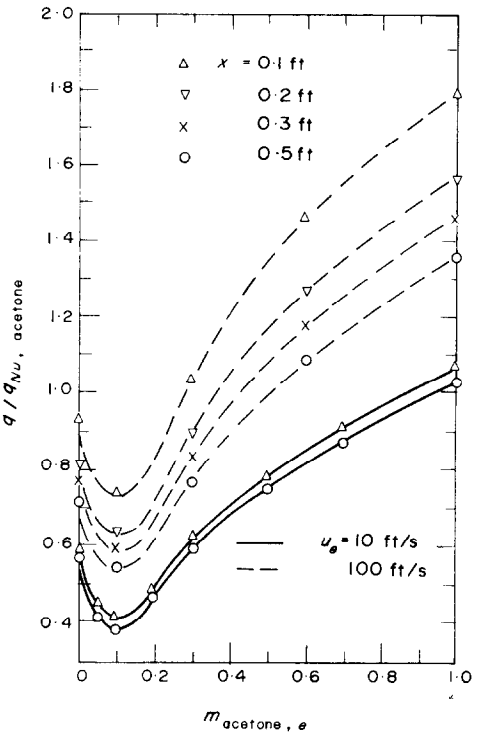

FIG. 10. Effects of $m_{1,e}$ and u_e on condensation of acetone–CCl_4 mixtures; $P_e = 300$ Torr, $T_e - T_w = 20°F$.

effect is not unlike that for the noncondensable gas problem [2, 3, 15] wherein accumulation of a noncondensing species at a pure condensate film surface leads to marked reductions in q/q_{Nu}. The severity of this "noncondensable gas effect" increases, of course, with relative volatility $\alpha = p_{sat,1}/p_{sat,2}$. However, unlike the noncondensable gas problem, condensation of mixed vapors is further complicated by the strong dependence of the aforementioned physical property ratio $(A/A_0)^{\frac{1}{4}}$ on $m_{1,u}(m_{1,s}, P_e)$.

Bearing the above in mind, interpretation of the effects of $m_{1,e}$ on q/q_{Nu} is straightforward. Thus, the initial behavior of $q/q_{Nu,H_2O}$ for aqueous mixtures of methanol and acetone is similar (Figs. 6–8) since the nearly 3-fold more rapid decline in $(T_i - T_w)$ with increasing $m_{1,s}$ for the former is balanced by a larger value of α (8·9 versus 4·3) and a more rapid reduction in $(A/A_0)^{\frac{1}{4}}$ for the latter. For propanol–water (Fig. 9), rapid reductions in $(A/A_0)^{\frac{1}{4}}$ with increasing $m_{1,u}$ are ameliorated by a small value of α (~ 1); while, for acetone–CCl_4 (Fig. 10),

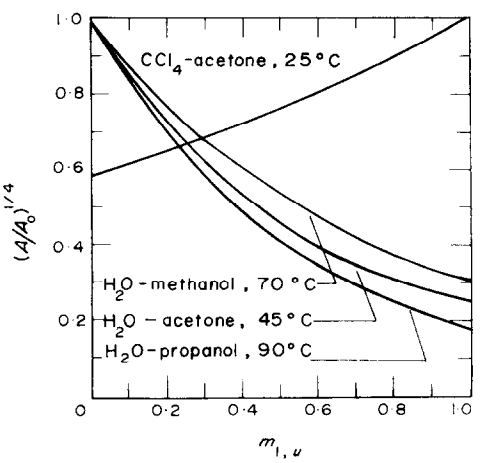

FIG. 11. Effects of liquid film composition on $A = k_l^3 \rho_l \lambda / \nu_l$.

strong reduction in $T_i - T_w$ with increasing $m_{1,s}$ are sharply compensated for by a modest value of α (~ 2) and *increasing* values of $(A/A_0)^{\ddagger}$.

The minima in q/q_{Nu} are dictated by equilibrium considerations; as $m_{1,e} \to 1$, the extent to which the more volatile species can accumulate at the interface is constrained ($m_{1,s} \leqslant 1$) and $(T_i - T_w)/(T_e - T_w) \to 1$. For acetone–$CCl_4$, the minimum occurs at reduced $m_{1,e}$ because T_i is essentially uniform for $m_{1,s} \geqslant 0{\cdot}5$ (see Fig. 2). Also, $q/q_{Nu,\,\text{acetone}}$ increases thereafter and surpasses its initial value because $(A/A_0)^{\ddagger}$ increases with increasing $m_{1,u}$ (Fig. 11). For acetone–water, q/q_{Nu} undergoes a second sharp reduction as $m_{1,e} \to 0{\cdot}7$. From Fig. 2, it is seen that, for $0{\cdot}6 < m_{1,e} \leqslant 0{\cdot}9$, $T_e - T_i \doteq T_e - T_w = 20°\text{F}$ (11·1°C). At $m_{1,e} = 0{\cdot}6$, for example, $T_i - T_w \doteq 0{\cdot}65°\text{F}$ when $T_e - T_w = 20°\text{F}$, $u_e = 10$ ft/s, and $x = 0{\cdot}5$ ft. As might be expected, the numerical technique described earlier experienced stability problems as $T_i \to T_w$. Thus, an "approximate" method was devised whereby the vapor-side problem is effectively decoupled from the liquid side problem by setting

$$T_e - T_i^* = \text{constant} = (T_e - T_w) - \varepsilon\,. \qquad (25)$$

a "best value" of ε being established iteratively by calculating

$$T_i(x) - T_w = -\dot{m}\lambda\delta(T_i^*)/k_l\,, \qquad (26)$$

where

$$\dot{m} = \rho\mathscr{D}_{12}\,\partial m_1/\partial y|_s/[m_{1,s}(T_i^*) - m_{1,u}(T_i^*)]\,. \qquad (27)$$

and imposing the constraint

$$\int_{x_0}^{x_L} (T_i^* - T_i)\,dx \doteq 0 \qquad (x_0 \sim 10^{-4}\ \text{ft}). \qquad (28)$$

For $(T_i - T_w)/(T_e - T_w) < 0{\cdot}05$, this approach results in only modest reductions in accuracy. For larger values, the approach is still satisfactory for engineering calculations. For example, Fig. 12 presents comparisons of results obtained in this way with the "exact" solution. Despite the fact $T_i - T_w$ as computed from equation (26) varies by a few degrees, the maximum error in q/q_{Nu} is still less than 10 per cent. Although T_i^* could be assigned as a monotonic decreasing function of x, this proved to be unnecessary in the present situation.

The absence of a minimum in q/q_{Nu} for propanol–water (Fig. 9) is due to the presence of an azeotrope at $m_{1,v} = 0{\cdot}718$. For $m_{1,e} > 0{\cdot}718$, *water* is the more volatile component and $m_{1,s} < m_{1,e}$. From Fig. 2, it is seen that $T_i - T_w$ therefore approaches $T_e - T_w$ as $m_{1,e} \to 1$ less rapidly than is the case for the non-azeotropic pairs. Since $(A/A_0)^{\ddagger}$ continues to decline as $m_{1,e} \to 1$, q/q_{Nu} decreases monotonically over the full range $0 \leqslant m_{1,e} \leqslant 1$.

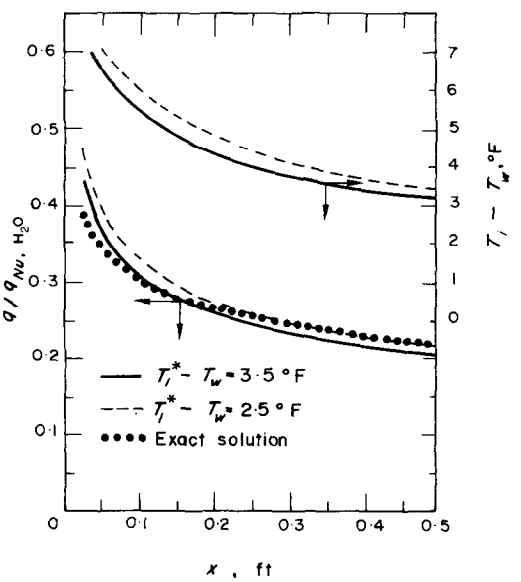

FIG. 12. Comparisons of decoupled solution technique with full numerical solution; acetone–water, $m_{1,e} = 0{\cdot}14$, $T_e - T_w = 20°\text{F}$, $u_e = 10$ ft/s.

Of added interest is the effect of forced flow on the location of $q/q_{Nu}|_{\min}$. For methanol–water (Fig. 6), it is seen that $m_{1,e}$ at $q/q_{Nu}|_{\min}$ shifts from $m_{1,e} \doteq 0{\cdot}43$ to $m_{1,e} \doteq 0{\cdot}65$ as u_e increases from 1 to 100 ft/s. This effect is due to enhancement of the mass transfer conductance

($\mathscr{g} \propto u_e^{\frac{1}{2}}$), which serves to ameliorate the effects of net accumulation of (more volatile) methanol at the s-surface. Thus, the deleterious effects of reductions in both $T_i - T_w$ and $(A/A_0)^{\frac{1}{2}}$ on q/q_{Nu} are less severe as u_e increases. Not unexpectedly, the effects of increasing u_e on the rate of shift in $m_{1,e}$ ($q/q_{Nu}|_{\min}$) are most pronounced at $u_e \to 0$. For acetone–CCl_4 (Fig. 10), the relative reductions in $m_{1,s} - m_{1,e}$ with increasing u_e also lead to increased values of $T_i - T_w$; such increases are opposed by decreased values of $(A/A_0)^{\frac{1}{2}}$ (Fig. 11) and the net effect is a negligible shift in $m_{1,e}(q/q_{Nu}|_{\min})$. For acetone–water (Fig. 8), the minima in q/q_{Nu} are so sharply defined by equilibrium considerations that negligible shift occurs.

Typical results for the effects of $T_e - T_w$ on q/q_{Nu} are presented in Fig. 7. It is seen that $m_{1,e}$ ($q/q_{Nu}|_{\min}$) as well as $q/q_{Nu}|_{\min}$ tend to increase with increasing $T_e - T_w$. Recalling equations (22) and (24), these trends are explained by the effects of increased suction on the mass-transfer conductance.

REFERENCES

1. E. M. SPARROW and E. MARSCHALL, Binary, gravity-flow film condensation, *J. Heat Transfer* **91**, 205–211 (1969).
2. V. E. DENNY, A. F. MILLS and V. J. JUSIONIS, Laminar film condensation from a steam–air mixture undergoing forced flow down a vertical surface, *J. Heat Transfer* **93**, 297–304 (1971).
3. V. E. DENNY and V. J. JUSIONIS, Effects of non-condensable gas and forced flow on laminar film condensation, *Int. J. Heat Mass Transfer* **15**, 315–326 (1972).
4. V. J. JUSIONIS, Effects of noncondensables, forced flow, and variable properties on film condensation of pure and binary vapors, Ph.D. dissertation, University of California, Los Angeles, 1971.
5. V. E. DENNY and A. F. MILLS, Nonsimilar solutions for laminar film condensation on a vertical surface, *Int. J. Heat Mass Transfer* **12**, 965–979 (1969).
6. S. V. PATANKAR and D. B. SPALDING, A finite difference procedure for solving the equations of the two dimensional boundary layer, *Int. J. Heat Mass Transfer* **10**, 1389–1411 (1967).
7. *Gleichgewichte Dampf-Kondensat und Osmotische Phänomene*. Landolt-Börnstein, *Zahlenwerte and Funktionen aus Physik, Chemie, Astromie, Geophysik, Technik, II.* Band, 2. Teil, Bandteil a, Springer-Verlag, Berlin (1969).
8. E. A. MASON and L. MONCHIK, Transport properties of polar gas mixtures, *J. Chem. Phys.* **36**, 2746–2757 (1962).
9. R. A. SVEHLA, Estimated viscosities and thermal conductivities at high temperatures, NASA-TR R-132 (1962).
10. R. A. SEBAN, Remarks on film condensation with turbulent flow, *Trans. Am. Soc. Mech. Engrs* **76**, 299 (1954).
11. W. M. ROHSENOW, J. H. WEBER and A. J. LING, Effect of vapor velocity on laminar and turbulent film condensation, *Trans. Am. Soc. Mech. Engrs* **78**, 1637 (1956).
12. S. S. KUTATELADZE, *Fundamentals of Heat Transfer*, pp. 289–326. Edward Arnold, London (1963).
13. A. ACRIVOS, Mass transfer in laminar-boundary-layer flows with finite interfacial velocites, *A.I.Ch.E. Jl* **6**, 410–414 (1960).
14. R. IGLISCH, Exact calculation of laminar boundary layer in longitudinal flow over a flat plate with homogeneous suction, NACA T.M. 1205 (1949).
15. W. J. MINKOWYCZ and E. M. SPARROW, Condensation heat transfer in the presence of noncondensables, interfacial resistance, superheating, variable properties, and diffusion, *Int. J. Heat Mass Transfer* **9**, 1125–1144 (1966).

EFFETS D'UN ECOULEMENT FORCE ET DES PROPRIETES VARIABLES SUR LA CONDENSATION D'UN FILM BINAIRE

Résumé—On présente l'analyse de la condensation en film laminaire de mélanges de vapeurs binaires qui s'écoulent en mouvement forcé vers le bas le long d'une plaque plane verticale. Les équations de conservation représentant le problème d'écoulement biphasique sont nettement non affines et sont résolues numériquement à l'aide d'une technique itérative. Le comportement du film liquide est traité au moyen d'une analyse du type Nusselt localement valable qui satisfait les conditions limites internes pour le problème du côté vapeur. Des propriétés localement variables dans la phase liquide sont obtenues à partir de résultats sur le mélange, les effets des variations de température à travers le film tombant étant évalués à des températures de référence appropriées. Les propriétés du mélange de vapeurs sont calculées à partir de la théorie cinétique.

Les résultats de transfert thermique donnés par le rapport q/q_{Nu} où q_{Nu} désigne la solution classique de Nusselt pour une des espèces pures, sont rapportées aux mélanges binaires méthanol–H_2O, propanol–H_2O, acétone–H_2O et acétone–CCl_4. Pour des mélanges binaires non azéotropiques on trouve que q/q_{Nu} passe par un minimum quand la concentration moyenne du composant le plus volatil augmente. L'approche

du minimum est semblable dans la solution du problème avec un gaz non condensable, la grandeur du rapport $q/q_{Nu\ mini}$ étant inversement proportionnelle à la volatilité relative de la paire binaire. Une seconde particularité de la condensation en film binaire est la nette dépendance de q/q_{Nu} vis à vis de la composition du film liquide à travers ses propriétés variables. Les effets de convection forcée sont semblables à ceux observés dans le problème du gaz non condensable.

DER EINFLUSS ERZWUNGENER STRÖMUNG UND VERÄNDERLICHER STOFFWERTE AUF BINÄRE FILMKONDENSATION

Zusammenfassung—Es werden Betrachtungten angestellt über die laminare Filmkondensation von binären Dampfgemischen bei abwärtsgerichteter Zwangsströmung an einer senkrechten ebenen Platte. Die Erhaltungssätze für dieses gekoppelte Zweiphasenproblem sind im wesentlichen unähnlich und wurden direkt numerisch gelöst.

Das Verhalten des flüssigen Films wurde mit Hilfe einer örtlich gültigen, Nusselt-artigen Betrachtung behandelt, die die inneren Randbedingungen für die Dampfseite bereitstellte, Die örtlich veränderlichen Stoffwerte der flüssigen Phase wurden aus Werten der Mischung berechnet. Der Einfluss der veränderlichen Temperatur quer zum fallenden Film wurde bei geeigneten Bezugstemperaturen berücksichtigt. Die Stoffwerte der Gasmischung wurden aus der kinetischen Theorie berechnet.

Die Ergebnisse des Wärmeübergangs in der Form q/q_{Nu}, wobei q_{Nu} die klassische Nusseltlösung für eine der beiden reinen Stoffe ist, werden für die binären Gemische Methanol-H_2O, Propanol-H_2O, Azeton-H_2O, und Azeton-CCl_4 aufgezeigt. Bei nicht azeotropischen binären Gemischen zeigt sich, dass q/q_{Nu} ein Minimum durchläuft, wenn die Freistromkonzentration des flüchtigeren Gases zunimmt. Die Annäherung an das Minimum ist im Charakter ähnlich dem Problem bei nichtkondensierbaren Gasen, wobei die Grösse von $q/q_{Nu\,min}$ umgekehrt proportional der relativen Flüchtigkeit des binären Stoffpaares ist. Eine zweite Eigenheit der Filmkondensation binärer Gemische ist die lineare Abhängigkeit der Werte q/q_{Nu} von der Zusammensetzung des flüssigen Films auf Grund der veränderlichen Flüssigkeitsstoffwerte. Die Einflüsse derZ wangskonvektion sind ähnlich den beobachteten bei dem Problem der nicht kondensierbaren Gase.

ВЛИЯНИЕ ВЫНУЖДЕННОГО ПОТОКА И ПЕРЕМЕННЫХ ТЕПЛОФИЗИЧЕСКИХ СВОЙСТВ НА ПЛЕНОЧНУЮ КОНДЕНСАЦИЮ

Аннотация—Проводится анализ ламинарной пленочной конденсации бинарных паровых смесей на вертикальной плоской пластине при вынужденном течении. Уравнения сохранения, описывающие сопряженную задачу двухфазного течения, неавтомодельны и решаются численным методом. Поведение жидкой пленки анализируется с позиций теории Нуссельта, в результате чего выводятся граничные условия задачи для паровой фазы. По данным для смеси определялись локальные значения свойств жидкой фазы, причем влияние изменений температуры по сечению падающей пленки оценивалось относительно соответствующей приведенной температуры. Свойства паровых смесей рассчитывались по кинетической теории газов.

Данные по теплообмену в виде зависимости q/q_{Nu}, где q_{Nu} -результат классического решения Нуссельта для однокомпонентной среды, представлены для бинарных смесей H_2O с метанолом, пропанолом, ацетоном, а также для смеси ацетон- CCl_4. Установлено, что для неазеотропных бинарных смесей q/q_{Nu} возрастает с увеличением объемной концентрации более летучего компонента. Тенденция к минимуму такая же, как в задаче о неконденсирующемся газе, причем величина $q/q_{Nu\ min}$ обратно пропорциональна относительной летучести бинарной пары. Вторым отличительным свойством бинарной пленочной конденсации является зависимость величины q/q_{Nu} от состава жидкой пленки вследствие переменности свойств жидкости. Влияние вынужденной конвекции сказывается также, как в случае неконденсирующегося газа.